Qin *et al. Bioresour. Bioprocess. (2018) 5:28*
https://doi.org/10.1186/s40643-018-0214-8

Bioresources and Bioprocessing

RESEARCH

Open Access

Light/dark cycle enhancement and energy consumption of tubular microalgal photobioreactors with discrete double inclined ribs

Chao Qin, Yuling Lei and Jing Wu*

Abstract

Tubular photobioreactors (PBRs) have a great potential in large-scale biomass cultivation and mixers in tubular PBRs have been intensively investigated to achieve high biomass productivity. However, mixers increase not only biomass yield, but also energy consumption. To evaluate performances on increasing light/dark (L/D) cycles and energy consumption of adding a mixer simultaneously, a new parameter named as efficiency of L/D cycle enhancement is introduced. Discrete double inclined ribs, intensively studied in heat transfer, are introduced to tubular PBRs in this work. The number of ribs in a cross section is discussed. These tubular PBRs are investigated in terms of the flow structure, L/D cycle frequency and efficiency of L/D cycle enhancement by computational fluid dynamics. The numerical results show that the increment of L/D cycle frequency caused by the discrete double inclined ribs is larger than the increment of energy consumption caused by the ribs under a wide range of incident light intensity. In general, the increasing of rib length ratio results in a decrease of efficiency and the PBR with two pairs of ribs performs the best. Based on the general trends, a PBR with two pairs of ribs and of which the rib length ratio is 5 is recommended for further studies.

Keywords: Tubular photobioreactor, Discrete double inclined ribs, Vortexes, Light/dark cycle, Efficiency of light/dark cycle enhancement

Introduction

Microalgae are a potential feedstock to produce biofuel (Wijffels and Barbosa 2010; Georgianna and Mayfield 2012). Currently, microalgae are cultivated in raceway ponds, which have the disadvantages of low productivity and risk of contamination (Georgianna and Mayfield 2012). In contrast, enclosed photobioreactors (PBRs) prevent microalgae from contamination, provide them a comfortable environment and thus achieve a continuous and high-yielding culture with high biomass concentration (Georgianna and Mayfield 2012). Among the types of PBRs, tubular PBRs have the potential for scaling up, due to their high surface-to-volume ratio and the ability to cultivate and harvest biomass continuously (Chisti 2008).

Easing light saturation and photoinhibition by light/dark (L/D) cycles is a way to increase biomass production. Cells with L/D cycles can grow faster and endure a higher biomass concentration for the so-called flashing light effect (Abu-Ghosh et al. 2016). Huang et al. (2014) have illustrated that L/D cycles, rather than turbulent kinetic energy or turbulent kinetic energy dissipation rate, is the parameter that directly relates to the biomass output by correlation analysis based on experiments and simulations. Also, light fluctuation is the main factor considered in a newly developed microalgal growth model (Gao et al. 2017).

L/D cycles can be achieved by mixers (Chisti 2008). Vortexes, induced by mixers, move suspension between the illuminated surface and the core center

*Correspondence: jingwu12@gmail.com
School of Energy and Power Engineering, Huazhong University of Science and Technology, Luoyu Road 1037, Wuhan 430074, China

(Gómez-Pérez et al. 2017; Wu et al. 2010) and, therefore, increase the L/D cycles experienced by cells (Perner-Nochta and Posten 2007; Luo and Al-Dahhan 2004). However, the adding of mixers also increases energy consumption (mainly pumping costs). For instance, according to Zhang et al. (2013), the simulated energy consumption (calculated by pressure drop) of the PBR with helical mixer was 0.3 J kg^{-1} m^{-1}, which was much higher than that of the smooth PBR (0.0136 J kg^{-1} m^{-1}). It means that the energy consumption has increased almost by 2106% on inserting of the helical mixer. By comparison, the productivity of *Chlorella* sp. increased by 37%, which is much lower than 2106%.

Several researches (Wu et al. 2010; Gómez-Pérez et al. 2015, 2017) have proposed novel mixers in tubular PBRs and tried to lower the energy consumption of mixers. For example, Wu et al. (2010) have proposed symmetric spiral grooves generating a pair of longitudinal vortexes to enhance the swirl flow of the tubular PBR. Gómez-Pérez et al. (2017) have proposed a twisted tube and Gómez-Pérez et al. (2015) have proposed a tube with circular groove to reduce the energy consumption of mixers. However, these mixers and PBRs enhanced the mixing at the cost of more energy consumption or saved energy with poorer mixing. Moreover, mixing performance in these researches is mostly evaluated by swirl number. It is noted that a flow with a high swirl number may not be a flow with a correspondingly high frequency of L/D cycles of cells. For example, a flow for which the swirl is far from the separating line of light and dark zones cannot contribute to L/D cycles.

In heat transfer enhancement, to achieve a better performance on heat flux under limited energy consumption, tubes with discrete double inclined ribs have been introduced to generate the theoretical optimal velocity field based on field synergy (Zheng et al. 2015; Meng et al. 2005; Meng 2003; Li et al. 2007). The velocity field induced by discrete double inclined ribs consists of six vortexes in a cross section, and these vortexes are located between the core region and the wall vicinity. The flow structure in this pipe is different from that in other types of tubular PBRs, such as PBRs with helical mixer, Kenics mixer, spiral tubular PBR and twisted tubular PBR, investigated by Gómez-Pérez et al. (2017), and a PBR with inclined porous mixer studied by Cheng et al. (2016), where the core area of the vortexes is near the center line of the pipe. This special flow structure in the pipes with discrete double inclined ribs enhances the convection between the wall vicinity and the core region more efficiently (Zheng et al. 2015). Considering that the light zone is usually near the wall and the dark zone usually contains the core region of the pipe in dense culture, this special flow structure may enhance the L/D cycles more efficiently.

For the above-mentioned reasons, this work introduces the discrete double inclined ribs to the tubular PBRs to increase the L/D cycles. The performance of PBRs with these ribs is comprehensively studied by computational fluid dynamics (CFD). The results show that PBRs with discrete double inclined ribs performed well in enhancing the L/D cycle of cells under a wide range of incident light intensity with a moderate energy loss. Also, the increment of L/D cycle frequency is larger than the increment of energy consumption, indicating that these types of ribs can own a great potential in upscaling. In addition, a parameter study about the length ratio and the number of ribs was also conducted.

PBRs

Figure 1 shows the geometry of the tubular ribs with discrete double inclined ribs. 3D models were constructed by Solidworks tools. The simulated tubular length is 1.55 m and the diameter of the tube is 50 mm. The rib width (W) is 6 mm, the rib height (t) is 3 mm, the inclination angle (α) is 37.5°, the rib pitch (P) is 30 mm, and the rib length $L = L^* \times W$, where L^* is the rib length ratio, a variable in this work.

In PBRs, the L/D cycles are determined by the light field and velocity field. In outdoors, light beams are usually parallel (they are assumed to be incident along the *-y* direction in this work as Cheng et al. 2016 have done). To study the influence of the position of vortexes along the light incident direction on the L/D cycle frequency, we propose two new structures—two pairs of ribs (Fig. 1c) and a pair of ribs (Fig. 1b) by removing the ribs from the opposite direction of the light transfer.

Numerical and evaluation models

Simulation models

Turbulent model

Turbulent flow is required in enclosed PBRs to meet mass transfer requirement and prevent cells from deposition (Perner-Nochta and Posten 2007; Acién Fernández et al. 2013), and an average velocity of 0.5 m s^{-1} is suggested for tubular PBRs (Molina et al. 2001; Perner-Nochta and Posten 2007). The suspension properties are set to the properties of water (Gómez-Pérez et al. 2017). The simulations of turbulent flow in tubes with discrete double inclined ribs have been intensively studied (Zheng et al. 2015; Meng 2003). Among these simulation models, SST k–ω model has been suggested by Zheng et al. (2015) for this geometry, because it is more reliable than the k–ε models and standard k–ω model with a deviation no more than 10% compared with experimental data reported by Meng (2003). Therefore, the SST k–ω model

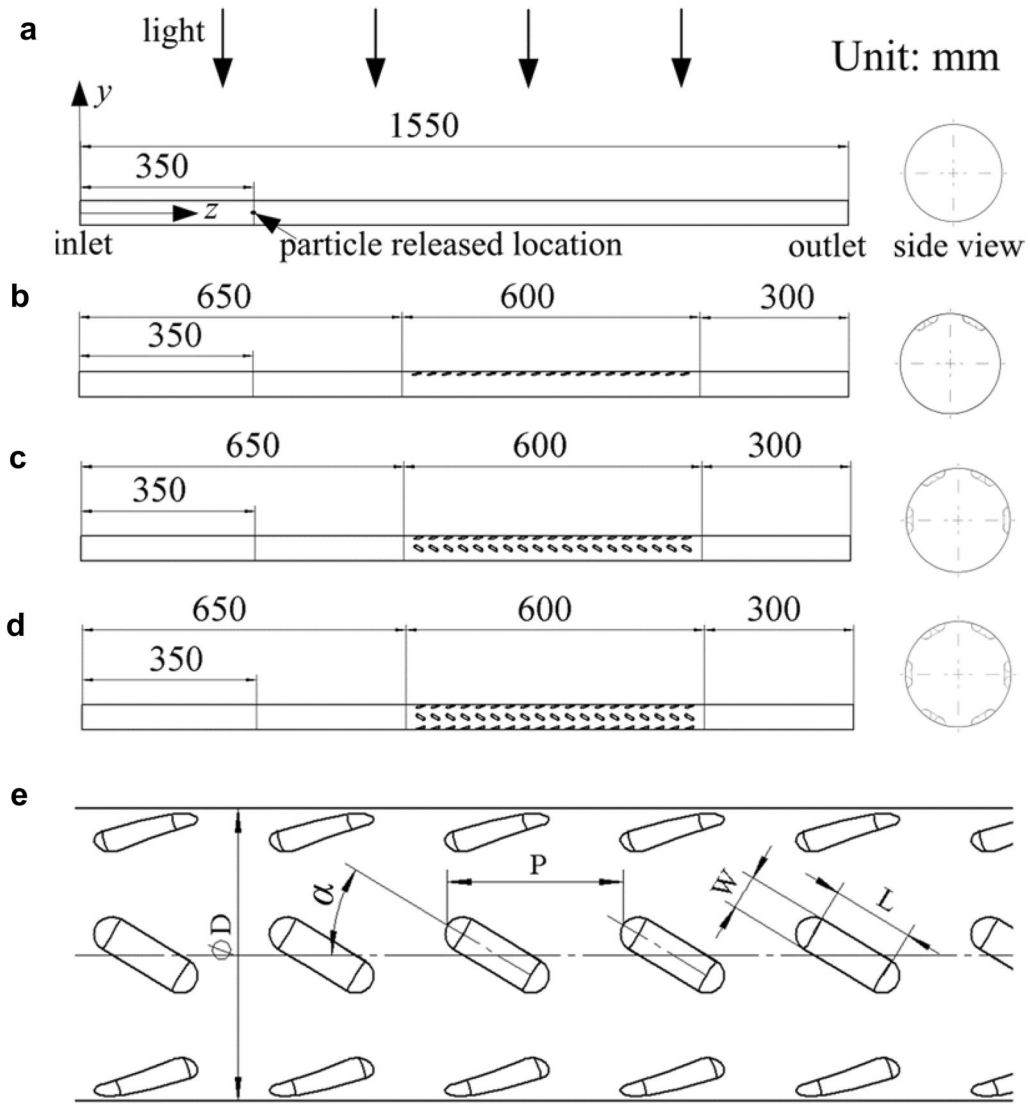

Fig. 1 **a** Smooth tubular PBR, named Type-0; **b** tubular PBR with a pair of ribs, named Type-1; **c** tubular PBR with two pairs of ribs, named Type-2; **d** tubular PBR with three pairs of ribs, named Type-3; **e** the detail of the ribs. Particles are released at $z = 0.35$ m of the tube center line where flow has been fully developed (Gómez-Pérez et al. 2015)

is selected in this work, and Fluent 14.0 is used to conduct this simulation. The governing equations are:

Continuity equation:

$$\frac{\partial u_i}{\partial x_i} = 0. \tag{1}$$

Momentum equation:

$$\rho \frac{\partial u_i u_j}{\partial x_j} = -\frac{\partial p}{\partial x_i} + \frac{\partial}{\partial x_j}\left[\mu\left(\frac{\partial u_i}{\partial x_j} - \rho\overline{u_i' u_j'}\right)\right]. \tag{2}$$

The turbulence kinetic energy equation:

$$\rho \frac{\partial k u_i}{\partial x_i} = \frac{\partial}{\partial x_j}\left[\left(\mu + \frac{\mu_t}{\sigma_k}\right)\frac{\partial k}{\partial x_j}\right] + \tilde{G}_k - Y_k + S_k. \tag{3}$$

The specific dissipation rate equation:

$$\rho \frac{\partial \omega u_j}{\partial x_j} = \frac{\partial}{\partial x_j}\left[\left(\mu + \frac{\mu_t}{\sigma_\omega}\right)\frac{\partial \omega}{\partial x_j}\right] + G_\omega - Y_\omega + D_\omega + S_\omega. \tag{4}$$

The constants for this model are:

$\sigma_{k,1} = 1.176$, $\sigma_{\omega,1} = 2.0$, $\sigma_{k,2} = 1.0$, $\sigma_{\omega,2} = 1.168$, $\alpha_1 = 0.31$, $\beta_{i,1} = 0.075$, $\beta_{i,2} = 0.0828$.

Particle tracking model

Microalgal cell movements are assumed to be the movement of particles, as in previous researches (Gómez-Pérez et al. 2015, 2017; Huang et al. 2014). The discrete random walk model was adopted to calculate the trajectories of particles (Yang et al. 2016; Perner-Nochta and Posten 2007). Particles in fluid are under the governing equation:

$$\frac{\mathrm{d}\vec{u}_\mathrm{p}}{\partial t} = F_\mathrm{D}(\vec{u} - \vec{u}_\mathrm{p}) + \frac{\vec{g}(\rho_\mathrm{p} - \rho)}{\rho_\mathrm{p}}, \tag{5}$$

where $\vec{u}$ is the fluid velocity, $\vec{u}_\mathrm{p}$ the particle velocity, ρ_p the particle density, ρ the fluid density and F_D the drag force coefficient.

Cells in the particle tracking model are usually assumed to be inert spheres (Pruvost et al. 2008; Gao et al. 2017), which are similar to the tracer used in particle tracking experiments conducted by Luo and Al-Dahhan (2004) and Pruvost et al. (2000). In this work, cells are assumed to be inert particles with a uniform diameter (10 μm) and density (1000 kg m^{-3}) (Moberg et al. 2012; Zhang et al. 2015). The virtual mass force and Saffman's lift force are neglected (Moberg et al. 2012; Perner-Nochta and Posten 2007). Tube surface is a reflective surface and the outlet is an escape one. Ten seconds are taken to be the maximum tracking time in this work and its independent validation is given in Additional file 1.

Light transfer model

The Cornet model is generally more appropriate than the Lambert–Beer model in the condition of high cell density culture (Acie et al. 1997). Thus, the Cornet model is selected to simulate the light profile in tubular PBRs in this work, which is expressed by

$$\frac{I}{I_0} = \frac{4\alpha_1}{(1+\alpha_1)^2 \cdot \mathrm{e}^{\alpha_2} - (1-\alpha_1)^2 \cdot \mathrm{e}^{-\alpha_2}}, \tag{6}$$

$$\alpha_1 = \sqrt{E_\mathrm{a}/(E_\mathrm{a} + E_\mathrm{s})}, \tag{7}$$

$$\alpha_2 = (E_\mathrm{a} + E_\mathrm{s}) \cdot \alpha_1 \cdot C_\mathrm{x} \cdot L, \tag{8}$$

$$L = \sqrt{r^2 - x^2} - y, \tag{9}$$

where I_0 and I are the incident and local light intensity, respectively, E_a and E_s are the mass absorption and scattering coefficients of algal cells, C_x is the biomass concentration and L is the light path. The constants in this work are $I_0 = 375$ μmol m^{-2} s^{-1} (Huang et al. 2014), 800 μmol m^{-2} s^{-1} (Perner-Nochta et al. 2007) and 1200 μmol m^{-2} s^{-1} (Zhang et al. 2013), $E_\mathrm{a} = 0.0014$ m^2 g^{-1}, $E_\mathrm{s} = 0.9022$ m^2 g^{-1} (for *Chlorella pyrenoidosa*, obtained by nonlinear fitting Huang et al. 2014) and $C_\mathrm{x} = 1.3$ g L^{-1} (a concentration in Huang et al. 2014).

Light is assumed to be incident along the *-y* direction (Fig. 1a) and transferring forward and backward only (Cheng et al. 2016). Tubes and mixers are assumed to be transparent and have no impact on light transfer (Cheng et al. 2016; Huang et al. 2014; Perner-Nochta and Posten 2007). The light profiles in PBRs calculated by Matlab are shown in Fig. 2.

Mixer performance

Statistic of the L/D cycle

The L/D cycle of individual cells can be calculated by the binary L/D pattern (Perner-Nochta and Posten 2007). The binary L/D pattern takes light field as the combination of the light zone and dark zone and ignores the light gradient within these two zones. The light zone is where the local light intensity is higher than the critical light intensity, and the dark zone is where the local light intensity is lower than the critical one (Perner-Nochta and Posten 2007; Luo and Al-Dahhan 2004). The critical light intensity, separating light and dark zone, is 96.84 μmol m^{-2} s^{-1} (Sorokin 1958; Huang et al. 2014) (Fig. 1).

A complete L/D cycle is defined as (Luo and Al-Dahhan 2004)

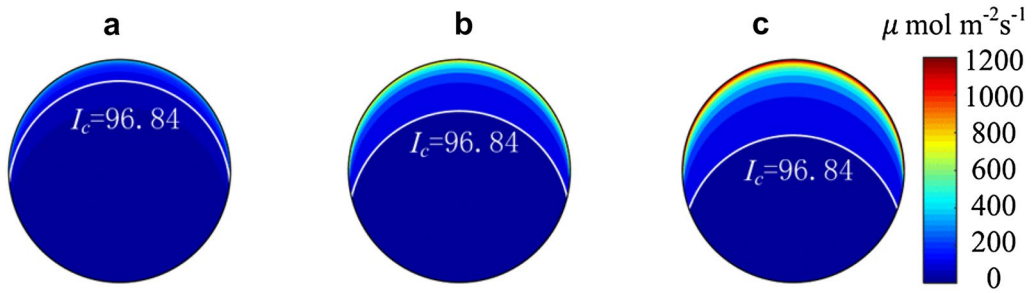

Fig. 2 Light profile for the incident light intensity of **a** 375 μmol m^{-2} s^{-1}, **b** 800 μmol m^{-2} s^{-1} and **c** 1200 μmol m^{-2} s^{-1}

$$t_c = t_d + t_l, \tag{10}$$

where t_d is the time that a particle stays in the dark zone and t_l in the light zone. The L/D cycle frequency is

$$f = 1/t_c. \tag{11}$$

An individual particle might experience a number of L/D cycles as it is moving back and forth between the light and dark zones continuously. For every particle, the average duration of L/D cycles is defined as

$$t_{c,av}^{ID} = \frac{\sum_1^n t_c}{n}, \tag{12}$$

where ID is the serial number of a particle and n is the number of L/D cycles of the particle.

The number of the particles should be large enough to ensure the reliability of the L/D frequency results (Huang et al. 2014), because the particle tracking model for an individual particle is based on the Gaussian probability distribution. In this work, 1000 particles are used as recommended by Huang et al. (2014) (the number validation is shown in Additional file 1). The average time of the L/D cycles of a group is (Huang et al. 2014)

$$t_{c,av} = \frac{\sum_{ID=1}^{ID=N} t_{c,av}^{ID}}{N}, \tag{13}$$

where N is the number of particles. Therefore, the averaged L/D cycle frequency is

$$f_{av} = 1/t_{c,av}. \tag{14}$$

Pressure drop

The average pressure at a cross section of the tubular PBR is (Gómez-Pérez et al. 2015)

$$P_{av} = \frac{\iint_S P ds}{S}, \tag{15}$$

where P is the local pressure and S is the area of the cross section.

The pressure drop between the outlet and the surface where particles are released is given by:

$$\Delta P = P_p - P_{out}, \tag{16}$$

where P_p is the average pressure at the surface where particles are released and P_{out} is the pressure of the outlet.

Efficiency of the L/D cycle enhancement

To evaluate the performance of the ribs on the L/D cycle enhancement and energy consumption simultaneously, we defined the efficiency of the L/D cycle enhancement in our previous work (submitted). The efficiency of the L/D cycle enhancement is the ratio of the dimensionless increment of the L/D cycle frequency to dimensionless increment of energy consumption per unit time, that is,

$$\eta = \frac{\Delta f_{av}/f_{av,0}}{\Delta E/E_0}, \tag{17}$$

where $f_{av,0}$ is the L/D cycle frequency of a smooth tubular PBR, $\Delta f_{av} = f_{av} - f_{av,0}$ is the increment of the L/D cycle frequency of PBRs with discrete double inclined ribs compared with the smooth PBR, $\Delta f_{av}/f_{av,0}$ is the dimensionless Δf_{av}, E_0 is the energy consumption of the smooth PBR, $\Delta E = E - E_0$ is the increment of energy consumption of PBRs with discrete double inclined ribs compared with the smooth PBR and $\Delta E/E_0$ is the dimensionless ΔE.

The energy consumption per unit time is (Gómez-Pérez et al. 2015)

$$E = \Phi \Delta P, \tag{18}$$

where Φ is the volume flow rate and ΔP the pressure drop. The diameters and average velocities of all the PBRs investigated in this work are the same, and thus the flow rate is the same. Then, we have $\Delta E/E_0 = (\Delta P - \Delta P_0)/\Delta P_0$ and the efficiency of the L/D cycle enhancement can be further expressed as

$$\eta = \frac{\Delta f_{av}/f_{av,0}}{(\Delta P - \Delta P_0)/\Delta P_0}. \tag{19}$$

Results and discussion

Validation of turbulent model

To confirm the reliability of the turbulent simulation procedure adopted in this work, the numerical results are compared with the experimental results reported by Meng (2003). Meng (2003) has tested the friction factor of a brass pipe with discrete double inclined ribs filled with deionized water and 22# lubricating oil, respectively. Here, the data of deionized water is chosen for comparison, since the property of microalgal suspension is similar to the deionized water. Detailed description of this experiment can be found in Meng (2003), Meng et al. (2005) (the experiments in these two papers were the same except that the media in the pipe studied in the latter was 22# lubricating oil only). As shown in Fig. 3, the trend of the simulation results of the friction factor (defined by Eq. 20) is well consistent with the experimental results, although there is still a deviation between them, which should be attributed to the uncertainty in experimental measurements and discrepancies between the numerical model and experimental model. Therefore,

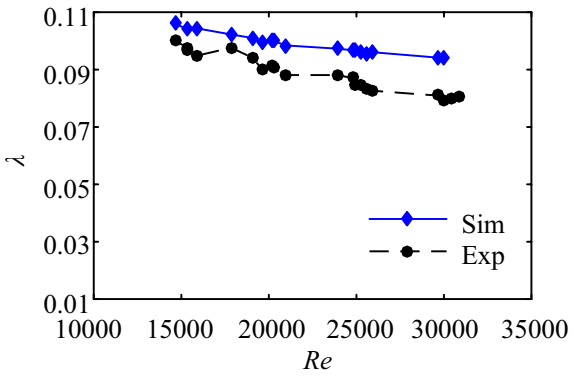

Fig. 3 Comparison between simulation and experimental results of friction factor; Sim represents the simulated results in this work, Exp represents the experimental results in Meng (2003)

it is reliable to use the numerical methods developed in this work. The friction factor (Meng 2003) is defined by

$$\lambda = \frac{2D\Delta p}{L\rho u^2}, \tag{20}$$

where u is the mean velocity in the tube.

Hydrodynamics and L/D cycle characteristics of tubular PBRs with discrete double inclined ribs

Flow structure

Prior to the discussion of the particle movements and L/D cycles, it is necessary to discuss the flow structure induced by inclined ribs. It is the flow structure that dominates the cell movements in PBRs. Figure 4 shows the tangential velocity and streamlines on a section between ribs ($L^*=3$). On the pathway formed by a pair of ribs, the tangential velocity vectors and streamlines head to the tube center, and thus a pair of vortexes forms on both sides of the pathway (Fig. 4c). This vortex structure is in good consistence with the visualization reported by Li et al. (2007), indicating the reliability of the turbulent model used in this work. These vortexes fill the cross section, and the number of vortexes is the same as the number of ribs at the cross section, indicating that an individual rib induces a vortex. The location of a vortex (Fig. 4c) corresponds to a rib at its upstream (Fig. 1d), which shows that the location of vortexes could be arranged by removing some ribs (Fig. 4a, b).

Particle tracks

Streamline and velocity vectors cannot show the particle mixing in PBRs directly, so the particle trajectories are presented in Fig. 5. We have tracked 1000 particles (ID number 0–999) and saved the position of each particle in

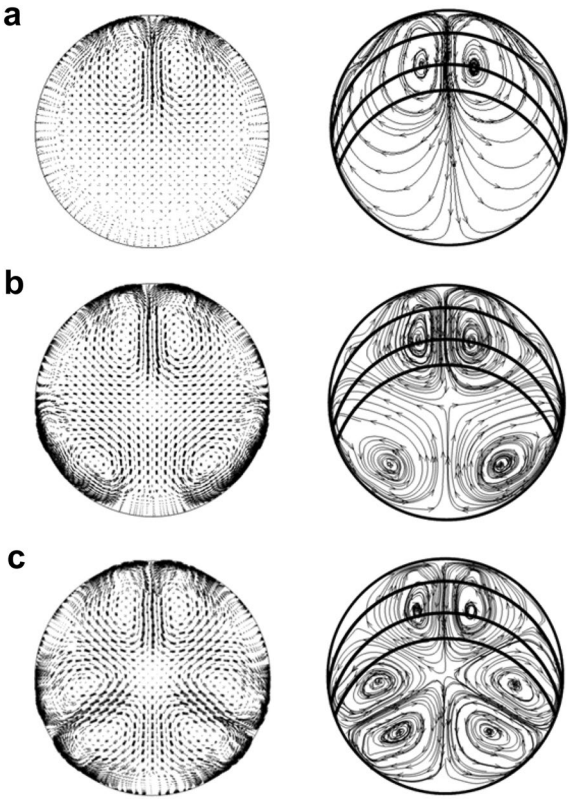

Fig. 4 Tangential velocity vectors and streamlines at section $z=905$ mm, **a** Type-1, **b** Type-2 and **c** Type-3; the solid lines in each streamline picture are critical light intensity when $I_0=375$, 800 and 1200 μmol m^{-2} s^{-1} from the top to center, respectively

sequence according to its resident time. For a clear view, the trajectories of 20 particles (ID number 0–19) among these tracked particles are drawn (plotted in Matlab) in Fig. 5. It can be seen that most particles could move across the entire cross section when ribs were added (Fig. 5a–c), while only a small fraction of particles could achieve that in the smooth PBR (Fig. 5d). As the number of the ribs and the rib length ratio, L^*, increases, particles move more strongly. It should be noticed that the particle movement caused by the increase of the rib length ratio is not as fierce as that caused by the increase of the rib number.

L/D cycle frequency

The average L/D cycle frequencies (f_{av}) are shown in Fig. 6. f_{av} tends to increase as the rib length ratio increases in these three types of PBRs. This trend coincides well with the particle trajectories trends.

However, f_{av} does not increase as the number of ribs increases. f_{av} of Type-2 is larger than that of Type-3 under three incident light intensities. This may be caused by the third pair of vortexes (Fig. 4c), located at the bottom of

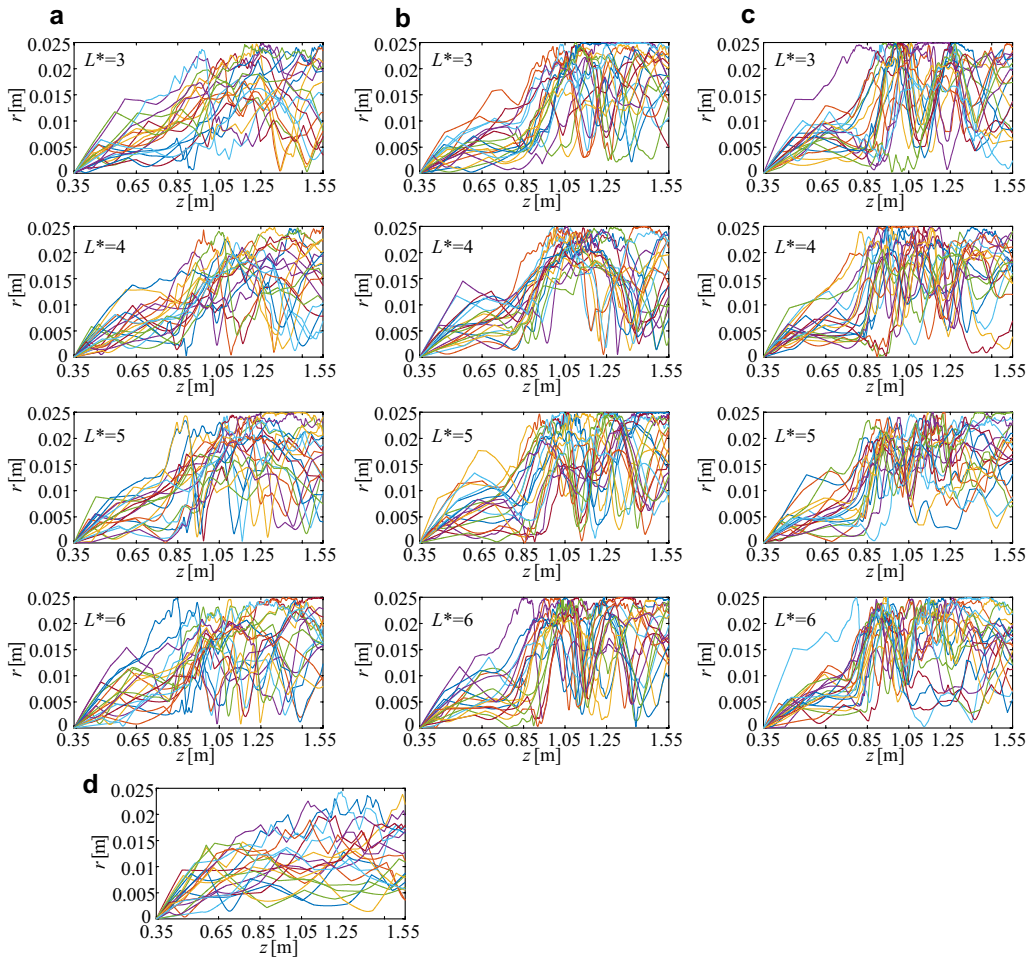

Fig. 5 The particle trajectories of **a** Type-1, **b** Type-2, **c** Type-3 and **d** Type-0

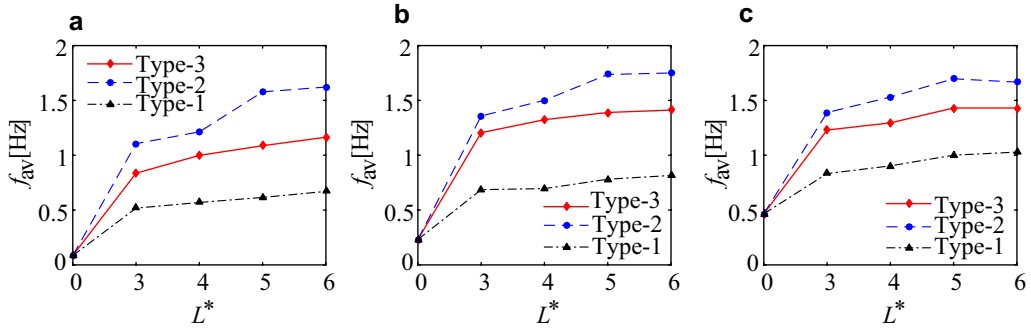

Fig. 6 Averaged L/D cycle frequency of three types of PBRs with different L^*. $L^*=0$ represents the PBR without ribs, i.e., the smooth PBR, which serves as a benchmark here; the incident light intensity is **a** 375 μmol m^{-2} s^{-1}, **b** 800 μmol m^{-2} s^{-1} and **c** 1200 μmol m^{-2} s^{-1}

the tube cross section. This pair of vortexes dominates the flow near it as other vortexes do, so the particle mixing of Type-3 is better than that of Type-2 since the former owns more vortexes. Moreover, the L/D frequency of Type-3 is lower than that of Type-2, because the third pair of vortexes of Type-3 is far from the separating line of light and dark zones, which means a large fraction of the particles of Type-3 is constrained in the bottom area without the L/D cycle.

As incident light intensity increases, f_{av} increases. A stronger incident light penetrates deeper, so that more particles can experience the L/D cycle. Meanwhile, the separating line of light and dark zones is not too far from the top vortex cores. Thus, a higher light intensity results in a higher f_{av}.

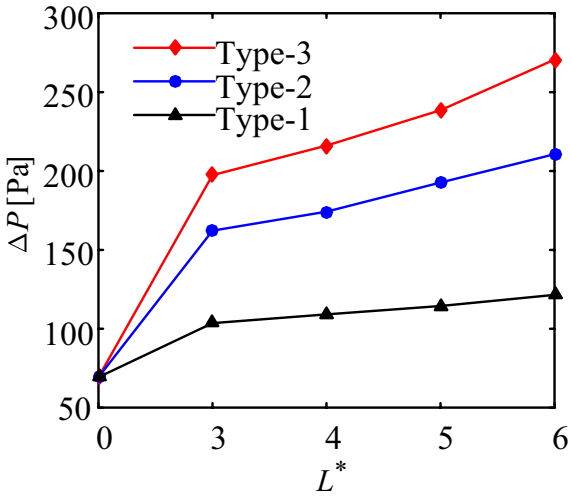

Fig. 7 Pressure drop of three types of PBRs with different L^*. $L^*=0$ represents the PBR without ribs, i.e., the smooth PBR, which serves as a benchmark here

Pressure drop

Pressure drop represents energy consumption in a tube with a constant cross-sectional area (Gómez-Pérez et al. 2017). The pressure drop increases as the rib length ratio, L^*, increases (Fig. 7). This is caused by the fact that a longer rib helps to induce a longer flow path around the ribs, resulting in a longer and stronger swirl flow, a better fluid mixing, and a greater flow blockage. Moreover, the pressure drop also increases as the number of ribs increases (Fig. 7). The increment of the pressure drop between different rib length ratios is not as large as that between different numbers of ribs. This trend is well consistent with the trend of particle trajectories, which indicates that stronger swirl flow could cause more particle movements across the entire cross section at a price of more energy consumption.

Efficiency of L/D cycle enhancement

The efficiency of L/D cycle enhancement is presented in Fig. 8. Almost all the efficiencies are higher than 1 (except the efficiencies of Type-3 under $I_0=1200$ μmol m^{-2} s^{-1} as shown in Fig. 8c), indicating that the increment of the L/D cycle frequency enhanced by discrete double inclined ribs is larger than that of the pressure drop caused by these ribs. It is worth noting that the efficiencies of the L/D cycle enhancement of most mixers which are currently used in other studies are less than 1. For instance, the efficiency of the L/D cycle enhancement of an inclined porous mixer proposed by Cheng et al. (2016) is only 4.45% (L/D cycle frequency increases from 1.69 to 3.13 Hz, while pressure loss increases from 25.85 to 520.64 Pa). As expected in the introduction part, the good performance of the discrete double inclined ribs on L/D cycle enhancement results from the special flow structure in this pipe.

Types-1 and -2 perform better than Type-3, and the efficiency of Type-1 is higher than that of Type-2 in most

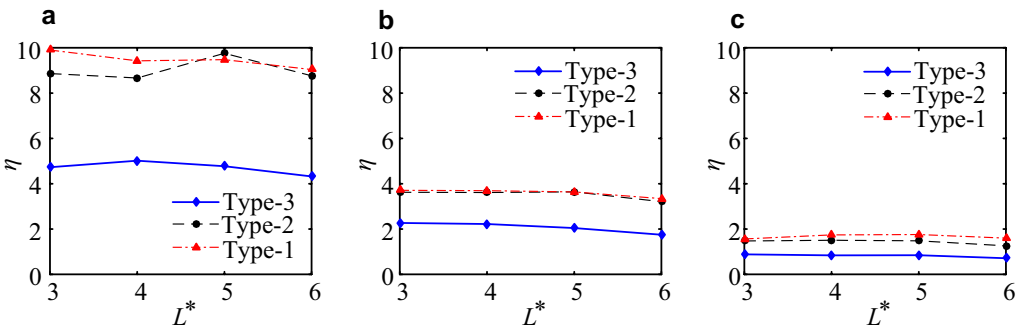

Fig. 8 The efficiency of L/D cycle enhancement of three types of PBRs with different L^*. The incident light intensities are **a** 375 μmol m^{-2} s^{-1}, **b** 800 μmol m^{-2} s^{-1} and **c** 1200 μmol m^{-2} s^{-1}

cases. As L^* increases, the efficiency shows a general decreasing trend. These two trends are consistent with usual cases that adding more mixers in a tubular PBR can bring the increases of mixing and pressure drop, but a decrease of efficiency. Considering the f_{av} of Type-2 is much higher than that of Type-1, and the efficiency of Type-1 is only slightly above that of Type-2, Type-2 should be used in cultivating. In a similar way, as the f_{av} increases with the increase of L^*, and the efficiency of $L^*=4$ or 5 performs the best in some cases, $L^*=4$ or 5 may be the optimal choice.

As shown in Fig. 8, Types-1 and -2 are efficient in enhancing L/D cycles under a wide range of incident light intensity. This feature is essential for outdoor cultivation because of the variation of sunlight (Pruvost et al. 2015). Namely, this type of PBRs has a potential for upscale cultivation of microalgae. It should be noticed that, as incident light intensity increases, the efficiency of the L/D cycle enhancement of each PBR decreases while f_{av} increases (as shown in "L/D cycle frequency" section). This decrease of efficiency may be because the benchmark ($L^*=0$ in Fig. 6) increases more than other PBRs do ($L^*=3$, 4, 5 and 6).

In addition, there might be some further studies that deserve attention. This work mainly focuses on numerical simulation and the results show that PBRs with discrete double inclined ribs perform well at enhancing L/D cycles. The biomass cultivation of species would be necessary to validate the advantages of this type of PBR. It will be conducted in the future. In particle trajectory simulation, cells in this work were taken as inert particles as in most researches (Huang et al. 2014; Gao et al. 2017; Pruvost et al. 2008; Zhang et al. 2013, 2015), while in real world particles are not (Suali and Sarbatly 2012; Razzak et al. 2013; Kreis et al. 2018). A more accurate particle tracking model including the shape and biological properties may present more detailed and accurate particle trajectories. However, it may result in a sharp increase of computing cost.

Conclusions

This work investigates the performance on enhancing L/D cycles and energy consumption of a tubular PBR with discrete double inclined ribs in dense culture. The special vortex structure in this type of PBRs enhances the L/D cycles efficiently as expected. In most cases (except Type-3 under $I_0=1200$ μmol m^{-2} s^{-1}), the efficiencies of L/D cycle enhancement are higher than 1, which means that the dimensionless increment of the L/D cycle frequency is larger than that of the pressure drop. Furthermore, the efficiencies of Types-1 and -2 are higher than 1 over a wide range of incident light intensity (from 375 to 1200 μmol m^{-2} s^{-1}), which indicates that Types-1 and -2 are more suitable for outdoor culture since the intensity of sunlight in nature varies with the time of the day.

As the number of ribs decreases from the opposite direction of the light transfer, the mixing performance of the cells decreases while the L/D cycle frequency does not (L/D cycle frequency is the highest when the number of ribs is 4, which corresponds to Type-2). This result indicates that a vortex far from the separating line of light and dark zones may reduce the L/D cycle, though it may increase the cell mixing. Furthermore, the pressure drop decreases as the number of ribs decreases. The efficiencies of L/D cycle enhancement of the PBR with four (Type-2) and two (Type-1) ribs are higher than that of PBR with six ribs (Type-3), while the difference in the efficiencies between Types-2 and -1 is slight. Considering that the L/D cycle frequency of Type-2 is much higher than that of Type-1, Type-2 possesses the best overall performance in our work and thus it is worthy of further investigation (including the real microalgal culture). As the rib length ratio increases, the pressure drop and averaged L/D cycle frequency increase while the efficiency shows a general decreasing trend. For Type-2, the efficiency of the L/D cycle enhancement is the highest in most cases when the rib length ratio equals 5. Thus, Type-2 with rib length ratio of 5 is recommended for further study.

Additional file

Additional file 1: Figure S1. Independent validation of maximum calculating time and verification of tracked particle number: (**a**) the number of particles escaped from outlet of the PBR under different maximum calculating time with 1000 particles released, and (**b**) the impact of number of released particles on f_{av} when the maximum calculating time is 10s.

Abbreviations

PBR: Photobioreactor; CFD: Computational fluid dynamics; L/D: Light/dark.

Authors' contributions

CQ: carried out the literature review, CFD and light profile simulations, analysis and interpretation of the data and drafting of the manuscript; YL: conducted CFD simulation; JW: contributed to the conception and design of the study, discussion of the results, critical revision of the manuscript for important intellectual content and obtaining of funding for the project. All authors read and approved the final manuscript.

Acknowledgements

Not applicable.

Competing interests

None declared.

Availability of data and materials

All data obtained in this study are presented in the manuscript. Raw data are available in the authors' group and can be provided if requested.

Consent for publication

Not applicable.

Ethics approval and consent to participate
Not applicable.

Funding
This research was supported by the National Natural Science Foundation of China (51576075).

Publisher's Note

Received: 20 March 2018 Accepted: 6 June 2018
Published online: 19 June 2018

References

Abu-Ghosh S, Fixler D, Dubinsky Z, Iluz D (2016) Flashing light in microalgae biotechnology. Bioresour Technol 203:357–363. https://doi.org/10.1016/j.biortech.2015.12.057

Acie FG, Sanchez JA, Grima EM (1997) A model for light distribution and average solar irradiance inside outdoor tubular photobioreactors for the microalgal mass culture. Biotechnol Bioeng 55:701–714

Acién Fernández FG, Fernández Sevilla JM, Molina Grima E (2013) Photobioreactors for the production of microalgae. Rev Environ Sci Biotechnol 12:131–151. https://doi.org/10.1007/s11157-012-9307-6

Cheng W, Huang J, Chen J (2016) Computational fluid dynamics simulation of mixing characteristics and light regime in tubular photobioreactors with novel static mixers. J Chem Technol Biotechnol. https://doi.org/10.1002/jctb.4560

Chisti Y (2008) Biodiesel from microalgae. Trends Biotechnol 26:126–131. https://doi.org/10.1016/j.tibtech.2007.12.002

Gao X, Kong B, Vigil RD (2017) Comprehensive computational model for combining fluid hydrodynamics, light transport and biomass growth in a Taylor vortex algal photobioreactor: Lagrangian approach. Bioresour Technol 224:523–530. https://doi.org/10.1016/j.biortech.2016.10.080

Georgianna DR, Mayfield SP (2012) Exploiting diversity and synthetic biology for the production of algal biofuels. Nature 488:329–335. https://doi.org/10.1038/nature11479

Gómez-Pérez CA, Espinosa J, Ruiz LCM, Van Boxtel AJB (2015) CFD simulation for reduced energy costs in tubular photobioreactors using wall turbulence promoters. Algal Res 12:1–9. https://doi.org/10.1016/j.algal.2015.07.011

Gómez-Pérez CA, Oviedo JJE, Ruiz LCM, Van Boxtel AJB (2017) Twisted tubular photobioreactor fluid dynamics evaluation for energy consumption minimization. Algal Res 27:65–72. https://doi.org/10.1016/j.algal.2017.08.019

Huang J, Li Y, Wan M et al (2014) Novel flat-plate photobioreactors for microalgae cultivation with special mixers to promote mixing along the light gradient. Bioresour Technol 159:8–16. https://doi.org/10.1016/j.biortech.2014.01.134

Kreis CT, Le Blay M, Linne C et al (2018) Adhesion of *Chlamydomonas* microalgae to surfaces is switchable by light. Nat Phys 14:45–49. https://doi.org/10.1038/nphys4258

Li X, Yan H, Meng J, Li Z (2007) Visualization of longitudinal vortex flow in an enhanced heat transfer tube. Exp Therm Fluid Sci 31:601–608. https://doi.org/10.1016/j.expthermflusci.2006.06.007

Luo HP, Al-Dahhan MH (2004) Analyzing and modeling of photobioreactors by combining first principles of physiology and hydrodynamics. Biotechnol Bioeng 85:382–393. https://doi.org/10.1002/bit.10831

Meng J (2003) Enhanced heat transfer technology of longitudinal vortices based on field-coordination principle and its application. Tsinghua University

Meng J, Liang X, Li Z (2005) Field synergy optimization and enhanced heat transfer by multi-longitudinal vortexes flow in tube. Int J Heat Mass Transf 48:3331–3337. https://doi.org/10.1016/j.ijheatmasstransfer.2005.02.035

Moberg AK, Ellem GK, Jameson GJ, Herbertson JG (2012) Simulated cell trajectories in a stratified gas–liquid flow tubular photobioreactor. J Appl Phycol. https://doi.org/10.1007/s10811-011-9765-1

Molina E, Fernández J, Acién FG, Chisti Y (2001) Tubular photobioreactor design for algal cultures. J Biotechnol 92:113–131. https://doi.org/10.1016/s0168-1656(01)00353-4

Perner-Nochta I, Posten C (2007) Simulations of light intensity variation in photobioreactors. J Biotechnol 131:276–285. https://doi.org/10.1016/j.jbiotec.2007.05.024

Perner-Nochta I, Lucumi A, Posten C (2007) Photoautotrophic cell and tissue culture in a tubular photobioreactor. Eng Life Sci 7:127–135. https://doi.org/10.1002/elsc.200620178

Pruvost J, Legrand J, Legentilhomme P, Doubliez L (2000) Particle image velocimetry investigation of the flow-field of a 3D turbulent annular swirling decaying flow induced by means of a tangential inlet. Exp Fluids 29:291–301. https://doi.org/10.1007/s003480000181

Pruvost J, Cornet JF, Legrand J (2008) Hydrodynamics influence on light conversion in photobioreactors: an energetically consistent analysis. Chem Eng Sci 63:3679–3694. https://doi.org/10.1016/j.ces.2008.04.026

Pruvost J, Cornet JF, Le Borgne F et al (2015) Theoretical investigation of microalgae culture in the light changing conditions of solar photobioreactor production and comparison with cyanobacteria. Algal Res 10:87–99. https://doi.org/10.1016/j.algal.2015.04.005

Razzak SA, Hossain MM, Lucky RA et al (2013) Integrated CO_2 capture, wastewater treatment and biofuel production by microalgae culturing—a review. Renew Sustain Energy Rev 27:622–653. https://doi.org/10.1016/j.rser.2013.05.063

Sorokin C, Krauss RW (1958) The effects of light intensity on the growth rates. Plant Physiol 33:109–113

Suali E, Sarbatly R (2012) Conversion of microalgae to biofuel. Renew Sustain Energy Rev 16:4316–4342. https://doi.org/10.1016/j.rser.2012.03.047

Wijffels RH, Barbosa MJ (2010) An outlook on microalgal biofuels. Science 329:796–799. https://doi.org/10.1126/science.1189003

Wu LB, Li Z, Song YZ (2010) Hydrodynamic conditions in designed spiral photobioreactors. Bioresour Technol 101:298–303. https://doi.org/10.1016/j.biortech.2009.08.005

Yang Z, Cheng J, Ye Q et al (2016) Decrease in light/dark cycle of microalgal cells with computational fluid dynamics simulation to improve microalgal growth in a raceway pond. Bioresour Technol 220:352–359. https://doi.org/10.1016/j.biortech.2016.08.094

Zhang Q, Wu X, Xue S et al (2013) Study of hydrodynamic characteristics in tubular photobioreactors. Bioprocess Biosyst Eng 36:143–150. https://doi.org/10.1007/s00449-012-0769-2

Zhang Q, Xue S, Yan C et al (2015) Installation of flow deflectors and wing baffles to reduce dead zone and enhance flashing light effect in an open raceway pond. Bioresour Technol 198:150–156. https://doi.org/10.1016/j.biortech.2015.08.144

Zheng N, Liu W, Liu Z et al (2015) A numerical study on heat transfer enhancement and the flow structure in a heat exchanger tube with discrete double inclined ribs. Appl Therm Eng 90:232–241. https://doi.org/10.1016/j.applthermaleng.2015.07.009